

# Mapping ebb tidal delta dynamics using Planet cubesat imagery within the Google Earth Engine

Murray R. Ford<sup>1</sup>, Mark E. Dickson<sup>1</sup> and Tom H. Durrant<sup>2</sup>

<sup>1</sup> University of Auckland, Auckland, New Zealand; [m.ford@auckland.ac.nz](mailto:m.ford@auckland.ac.nz)

<sup>2</sup> Oceanum Ltd., Raglan, New Zealand

## Abstract

The recent development of relatively low-cost Earth observation satellites now provides the ability to image the entire Earth's surface at daily timescales. Such high-cadence imagery has unlocked the ability to examine a range of processes at spatial and temporal scales previously inaccessible within coastal science. Here we present details on the use of imagery from the Planet Labs constellation of Earth observation satellites to examine changes on the Whāingaroa (Raglan) Harbour ebb tidal delta on the west coast of the North Island of New Zealand. The time-averaging of stacks of still images captured by oblique land-based cameras has been widely used to identify features such as rip channels, nearshore bars, ebb-tidal delta bars and channels, among others. Recently, a similar method has been developed to work with collections of satellite imagery from a range of government and commercial satellite sensors. By accessing 194 cloud-free images from 2017-2019 we are able to time-average collections of Planet Labs imagery with the Google Earth Engine (GEE), a cloud-based geospatial analytics platform. Using this approach, we can quantify the migration of bars and the main channel at the Raglan ebb tidal delta. Additionally, outputs of a high-resolution (5 km) wave hindcast of New Zealand waters and local tidal predictions were used to determine the wave conditions and water level at the time each image was captured enabling us to examine tidal and wave control on patterns of wave breaking. The approach we use is simple and with the growing constellations of commercial and government Earth observation satellites has a range of potential applications within coastal dynamics and maritime safety.

*Keywords: Ebb-tidal deltas, remote sensing, satellite imagery, Google Earth Engine*

## 1. Introduction

Ebb-tidal deltas are found fronting many of Aotearoa/NZ's harbours. These deltas are comprised of large volumes of sand which form dynamic bar and channel systems [1]. The deltas are key controls on coastal change by modulating alongshore sediment delivery which drives downdrift coastal change. Additionally, the shallow waters and energetic waves within delta systems make them a navigation hazard for vessel operators and have been the site of many of NZ's most deadly maritime accidents. Due to the shallow water, rapidly changing bathymetry, strong tidal flows and complex patterns of wave breaking ETD are particularly dangerous and expensive locations to gather *in situ* observations. Despite these challenges, hydrographic surveys and field observations of ETD are still undertaken alongside remote sensing and numerical modelling to resolve ETD dynamics [2-4].

Remote sensing studies of ETD have typically utilised imagery from ground-based [2,5], airborne [6] and spaceborne sensors [7-8] to successfully examine ETD dynamics. Ground-based cameras, such as those within the Argus or the Cam-Era systems, have been widely used to examine nearshore processes including rip detection [9], ETD dynamics [5] and bar migration [10] based on the contrast between broken (bright) and unbroken waves (dark) in digital images. When stacks of images are time-averaged areas of persistent broken and unbroken water become increasingly

evident. Such techniques are often used to indicate the presence of rips where wave breaking is relatively low compared to areas adjacent to the rip channel, resulting in time-averaged pixels which appear dark in a greyscale image. Conversely, shallow water over bars forces wave breaking resulting in highly reflective surface which appears white in a greyscale image.

Recently, this technique has been adapted for satellite imagery and applied at ETDs. Ford and Dickson [7] time-averaged imagery captured by the Landsat 7 and 8 satellites of the Manukau Harbour ETD on the west coast of Auckland, New Zealand and were able to observed migration of the bars and channels of >1 km on decadal timescales. Both Landsat 7 and 8 capture 15-30 m resolution imagery of the same location every 16 days, or 8 days in locations where orbital paths overlap. Ford and Dickson [8] addressed the limitation of Landsat imagery by utilising commercial imagery from Planet Inc. whose satellites capture 3-4 m imagery with a near-daily revisit time. A key weakness of these previous studies is that the approach does not consider the differences in water level or wave heights at the time of image capture and can therefore bias a record depending on the conditions at the time of image capture. For example, optical imagery is dependent on cloud-free conditions which are more frequent during summer months, therefore these image collections are likely biased toward periods of lower wave heights during summer. Likewise, the ability to examine the

patterns of wave breaking on ETD bars under different water levels and wave conditions provides the potential to develop tools to predict patterns of wave breaking at ETD's. Here we present details of the use of imagery from Planet Inc. coupled with water level and wave conditions at the time of image capture to examine the dynamics of the ETD at Raglan/Whāingaroa harbour on the west coast of the North Island of New Zealand.

## 2. Field Setting

Whāingaroa/Raglan Harbour on the west coast of the North Island of New Zealand (Figure 1). The harbour is part of a post-glacial drowned river valley [11]. The harbour is shallow, with an average depth of 2.5 m and a maximum depth of only 18 m. Of the harbours ~33 km<sup>2</sup> area ~24 km<sup>2</sup> is intertidal. The Raglan ebb-tidal delta (RETD) complex sits at the mouth of the harbour. The RETD is comprised of a shallow (<4 m) swash platform which extends ~2 km offshore from the inlet and is ~3 km wide [5] The delta is intersected by a channel oriented approximately east-west and ~300 m wide [5].

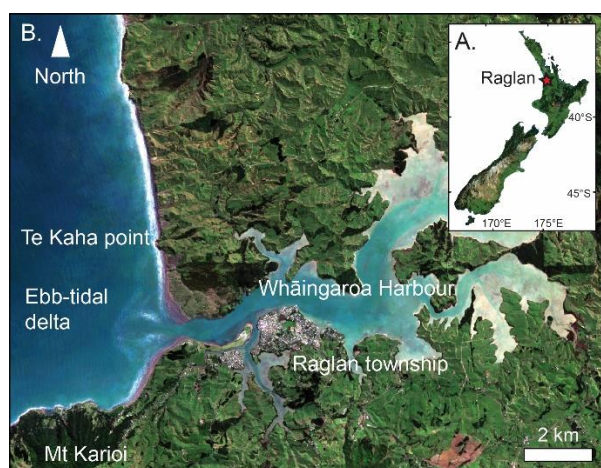


Figure 1 A & B) The Raglan ebb-tidal delta at the mouth of Whāingaroa (Raglan) Harbour on the west coast of the North Island of New Zealand.

## 3. Method

### 3.1 Planet satellite imagery

Planet Inc. is a US-based private company which operates the World's largest constellation of Earth Observation (EO) satellites [12]. Unlike traditional EO satellite systems which rely on a small number of large satellites the Planet constellation consists of >100 small 3U 'Dove' cubesats (i.e. 3 x 10cm<sup>3</sup>). Collectively, the active constellation of dove satellites enables near-daily imaging of the entire Earth's surface. Freely available imagery from government operated EO satellites, such as Landsat and Sentinel-2, have spatial resolutions between 10 and 30 m. In contrast, the best available spatial resolution of very high resolution (VHR) optical satellites is 30 cm, although these resolutions are only available in the panchromatic band which captures light from a broad spectrum,

rather than the multispectral bands (i.e. red, green, blue, NIR etc) which are typically 1-2 m in resolution. The spatial resolution from the Planet constellation is ~3.7 m, fitting between that of the freely available government EO data and that from VHR commercial satellites. Planet satellites collect imagery in a number of 'channels' or spectral bands. Early Planet satellites collected only visual bands (i.e. red, green and blue), whereas more recent iterations of the Dove satellites also collect a near-infrared band and some "super dove" satellites capture 8-band imagery at ~3.7 m resolution.

Planet deliver imagery at several different processing and calibration levels depending on the use of the imagery [12]. In this study we utilised the PlanetScope Ortho Tile product which has been orthorectified, geometrically and radiometrically calibrated and in units of at sensor radiance. All imagery we used were first inspected for cloud contamination prior to downloading. Images were subsequently converted into units of Top-of-Atmosphere (TOA) reflectance, which is intended to minimise differences between images collected at different levels of solar radiance (Figure 2).



Figure 2 True colour PlanetScope Ortho Tile image of the Raglan ebb-tidal delta captured 24-Feb-2019 showing the main channel, swash bars, channel margin linear bars and breaking on the terminal lobe ( $H_s = 3.02$  m and water level = 0.97 m).

### 3.2 Oceanographic conditions

To examine tidal and wave controls on the patterns of breaking on the RETD the water level relative to chart datum and incident wave height at the time of image capture were added as metadata properties to each image. This enables the collection of images to be filtered based on date, water level and wave height. Water level was calculated based on Land Information New Zealand (LINZ) tidal

predictions for Raglan, with the water level calculated at the time of image capture following calculations provided by LINZ (for full details see: <https://www.linz.govt.nz/sea/tides/tide-predictions/how-calculate-tide-times-heights>).

A three-hourly time series of significant wave height ( $H_s$ ) ~10 km offshore of the RETD was generated from a wave hindcast. The hindcast is produced by Oceanum Ltd. using the SWAN (Simulating Waves Nearshore) spectral wave model [13]. The model has been run for New Zealand coastal waters at a 5 km resolution and is forced with ERA5 winds and full spectral wave boundaries from a global wave model run by Oceanum Ltd. The wave height at the time of image capture was calculated by linearly interpolating between the wave heights preceding and proceeding image capture.

### 3.3 Data processing

We used the Google Earth Engine (GEE) to process the PlanetScope TOA imagery. The GEE is a cloud-based application for geospatial data analysis [14]. GEE provides access to a wide range of remote sensing algorithms which are run on Google's servers, negating the need for high-performance local computing. The GEE has been used to study a wide range of environments and processes in the coastal zone including: shoreline change [15], mangroves [16], coral reef islands [17] and ebb-tidal delta dynamics [7-8]. Users can access the GEE through a web-based code editor, which we used in this study, or can be accessed via a Python API.

Within GEE a stack of imagery is referred to as an image collection. Users can access existing image collections of freely available imagery within GEE (i.e. Landsat, Sentinel-2 and others) or can create their own image collections stored within GEE. All PlanetScope TOA imagery used in this study were uploaded into GEE with metadata containing the date and time of image capture along with the water level and wave height at the time of image capture. The imagery was then loaded into an image collection. The resultant collection comprised 194 images captured by between 01/01/2017 and 31/12/2019.

A range of summary statistics can be calculated from an image collection on a per-pixel basis through an image collection. Within GEE these operations are known as image reductions, where a collection of images is reduced to a single output image. Many of the common image reductions (i.e. mean, median and standard deviation) are analogous to methods applied to stacks of imagery from terrestrial images captured by the likes of Argus or Cam-era systems. Within GEE we derived the mean, median and standard deviation through the collection of images of the RETD (Figure 3). Given each image within the collection had

metadata fields for date/time, water level and wave height we were able to filter the collection of images based on these properties prior to running the image reductions. For example, we can time-average all images in a certain date range or those within a certain water level or range of wave heights.

## 4. Results

### 4.1 Identifying geomorphic features

The key features of the RETD were able to be readily identified in the mean, median and standard deviation reductions of the 2017-2019 image collection. The mean and median reduction clearly shows persistent breaking on the channel margin linear bars, swash bars and along the beach. Conversely, both reductions clearly show the absence of breaking in deep water offshore, within the main channel and within the sheltered waters within the harbour.

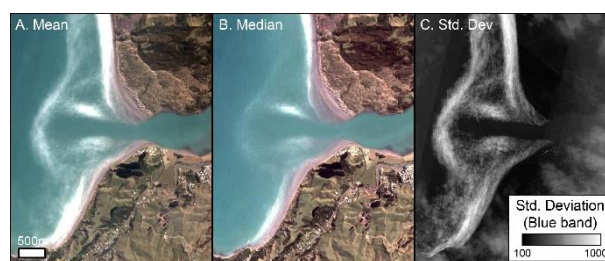


Figure 3 Mean (A), median (B) and standard deviation (C) reductions through the entire image collection. Note, the standard deviation is calculated for all bands, but for clarity is presented for only the blue band.

### 4.2 Change detection

Subtracting the mean reduction of the 2017 collection (Figure 4A) from the mean reduction of 2019 data (Figure 4B) reveals changes in the pattern of wave breaking on the RETD (Figure 4C). Of note, we observed a potential seaward shift of ~200 m in the position of the terminal lobe. Likewise, changes in the orientation of some of the channel margin linear bars are observed, resulting a clockwise rotation of the RETD. In general, the position of the main channel remained largely stable across these time periods.

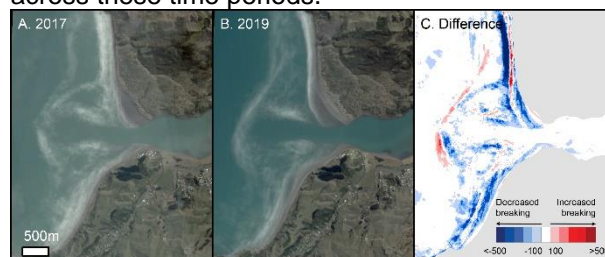


Figure 4 Mean reduction of all A) 2017 imagery and B) 2019 imagery and the difference in the image intensity (i.e. 2019-2017) in top of atmosphere reflectance values revealing areas of increased (red) and decrease (blue) reflectance indicating changes in wave breaking.

### 4.3 Wave and tide controls on wave breaking

In order to examine tidal and wave controls on breaking, the image collection was filtered into nine sub-collections based on water level and wave height and each sub-collection time-averaged. Each of the nine filtered collections contained a combination of the highest, middle, or lowest one-third of water levels and wave heights from the time of image capture. This enables the patterns of wave breaking on the RETD to be observed under different oceanographic conditions. When water levels were high (i.e. images captured during the highest one-third of water levels) and wave heights were low (i.e. images captured during the lowest one-third of wave conditions) waves are rarely observed to be breaking on the channel margin linear bars (CMLB), terminal lobe or swash bars (Figure 5A). Likewise the surf zone on the beaches adjacent to the channel are narrow, indicating limited breaking on the bars with only small waves (<0.99 m offshore) breaking directly on the beach face. Conversely, when water levels are low (lowest third) and wave heights are within the highest third (>2.51 m offshore) we observe extensive breaking across the terminal lobe and on all bars types (Figure 5I).

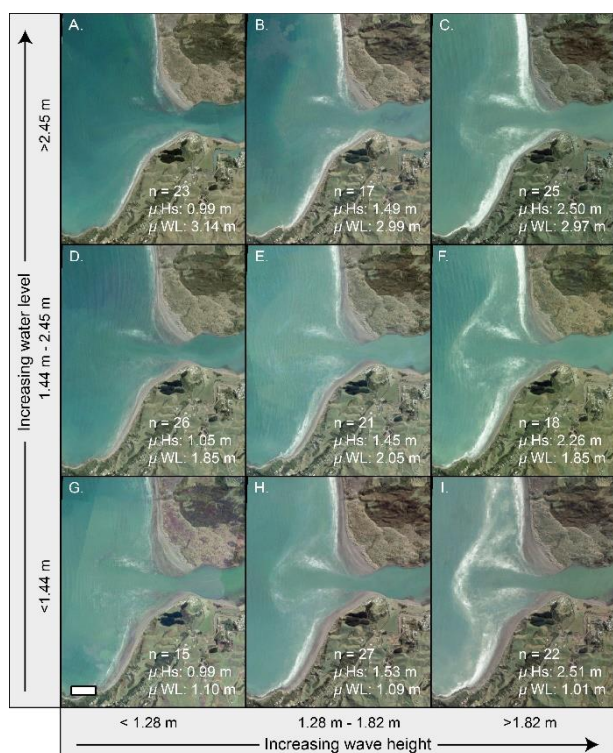


Figure 5 Mean image reductions of collections of PlanetScope TOA imagery from 2017-2019 filtered into the highest, middle and lowest one-third of water levels and wave heights.

## 5. Discussion

By accessing nearly 200 cloud-free, images from the Planet constellation of Earth observation satellites we are able to time-average the collection

to reveal patterns of wave breaking on the Raglan ebb-tidal delta. The contrast between broken (i.e. highly reflective pixels) and unbroken (i.e. dark pixels) makes identifying bars and channels straightforward. The ability to automate the analysis of such a rich collection of imagery using the Google Earth Engine makes such analysis scalable and without the need for significant local computing resources.

The technique we have developed is similar to those that have been used for decades to examine nearshore processes using fixed terrestrial cameras [5,9]. However, the approach has many key differences to those applied to oblique imagery from ground-based cameras. First, the imagery from the Planet constellation provides near-daily global coverage. The global coverage of satellite imagery provides opportunities to examine processes occurring over large spatial scales and in locations not accessible through ground cameras. Likewise, ground-based cameras are most effective when elevated to provide less acute viewing angles, whereas satellite imagery is near-nadir view of any section of the coast. Second, unlike ground-based cameras, satellite imagery provides a uniform resolution across the scene in contrast to ground-based cameras which show more detail in the foreground which limits their utility for examining large-scale features. Several other factors such as harmonised image processing (i.e. geometric and radiometric calibration) streamline image analysis, while rich archives of Planet imagery which now extend several years making analysis of new sites readily available. Conversely, there are several limitations in the use of optical satellite imagery which is often hampered by cloud-cover which reducing the number of useable images, particularly during winter months. As a result, our collection of imagery is biased towards summer months, when wave conditions are less energetic.

A key advance in our study is the inclusion of water level and wave height at the time of image capture which enables us to examine ebb-tidal delta dynamics under different forcing conditions (Figure 5). The ability to couple imagery with oceanographic conditions provides the opportunity to examine changes in ebb-tidal delta morphology in response to episodic and seasonal changes in wave conditions. Likewise, the coupled collection of imagery and water level and wave heights has the potential to be used to develop models to predict wave breaking on the RETD and potentially provide safety tools for vessels navigating complex ETD bar/channel systems.

### 5.1 Future opportunities

Imagery from the Planet constellation is one of several sources of imagery now available from either commercial or government satellites. By

including freely available imagery from government satellites including Sentinel 2 and Landsat it possible to increase the number of observations substantially, albeit at lower resolutions. Likewise, a number of new commercial satellites have been launched or are in development, providing opportunities to further improve the sampling frequency. Some platforms now capture short (<180 sec.) video from space which would enable the examination of short-term processes including wave breaking and runup.

### Summary

Using a rich collection of medium resolution optical satellite imagery from the Planet constellation of Earth observation satellites we mapped patterns of wave breaking on the Raglan ebb-tidal delta. We coupled outputs of wave and tidal models with the image collection to provide the water level and wave heights at the time of image capture enabling examination of the pattern of wave breaking under different conditions. The technique we have developed and presented has considerable potential to further understanding of ebb-tidal delta dynamics and develop tools for improving safety of vessels operating in ebb-tidal delta fronted harbours.

### 6. References

- [1] Fitzgerald, D.M. (1984), Interactions between the ebb-tidal delta and landward shoreline; Price Inlet, South Carolina, *Journal of Sedimentary Research*, vol. 54, no. 4, pp. 1303-1318. <https://doi.org/10.1306/212F85C6-2B24-11D7-8648000102C1865D>
- [2] Balouin, Y., Morris, B.D., Davidson, M.A. and Howa, H. (2004), Morphology evolution of an ebb-tidal delta following a storm perturbation: assessments from remote sensed video data and direct surveys, *Journal of Coastal Research*, pp. 415-423. 20 (2), 415–423. [https://doi.org/10.2112/1551-5036\(2004\)020\[0415:MEOAED\]2.0.CO;2](https://doi.org/10.2112/1551-5036(2004)020[0415:MEOAED]2.0.CO;2).
- [3] Elias, E.P. and van der Spek, Ad JF (2006), "Long-term morphodynamic evolution of Texel Inlet and its ebb-tidal delta (The Netherlands)", *Marine Geology*, vol. 225, no. 1-4, pp. 5-21. <https://doi.org/10.1016/j.margeo.2005.09.008>
- [4] Van Leeuwen, S.M., Van der Vegt, M. and De Swart, H.E. (2003), Morphodynamics of ebb-tidal deltas: a model approach, *Estuarine, Coastal and Shelf Science*, vol. 57, no. 5, pp. 899-907. [https://doi.org/10.1016/S0272-7714\(02\)00420-1](https://doi.org/10.1016/S0272-7714(02)00420-1)
- [5] Harrison, S.R., Bryan, K.R. and Mullarney, J.C. (2017), Observations of morphological change at an ebb-tidal delta, *Marine Geology*, vol. 385, pp. 131-145. <https://doi.org/10.1016/j.margeo.2016.12.010>
- [6] Hicks, D.M. and Hume, T.M. (1996), Morphology and size of ebb tidal deltas at natural inlets on open-sea and pocket-bay coasts, North Island, New Zealand, *Journal of Coastal Research*, vol. 12, no. 1, pp. 47-63.
- [7] Ford, M.R. and Dickson, M.E. (2018), "Detecting ebb-tidal delta migration using Landsat imagery", *Marine Geology*, vol. 405, pp. 38-46. <https://doi.org/10.1016/j.margeo.2018.08.002>
- [8] Ford, M.R. and Dickson, M.E. (2019) The use of Planet cubesat imagery to examine ebb-tidal delta dynamics. *Coastal Sediments 2019: Proceedings of the 9th International Conference*, pp. 2500-2510 [https://doi.org/10.1142/9789811204487\\_0215](https://doi.org/10.1142/9789811204487_0215)
- [9] Gallop, S.L., Bryan, K.R. and Coco, G. (2009) Video observations of rip currents on an embayed beach, *Journal of Coastal Research*, Proceeding of the 10th International Coastal Symposium, pp. 49-53.
- [10] Lippmann, T.C. and Holman, R.A. (1989), "Quantification of sand bar morphology: A video technique based on wave dissipation", *Journal of Geophysical Research*, vol. 94. no. 1, pp. 995-1011
- [11] Sherwood, A.M., and Campbell S.N. (1979) Surficial sediments of Raglan harbour. *New Zealand Journal of Marine and Freshwater Research* 13.4 (1979): 475-496.
- [12] Planet, Team. (2021) Planet application program interface: In space for life on Earth. San Francisco, CA [https://assets.planet.com/docs/Planet\\_Combined\\_Image\\_Ry\\_Product\\_Specs\\_letter\\_screen.pdf](https://assets.planet.com/docs/Planet_Combined_Image_Ry_Product_Specs_letter_screen.pdf) (last accessed 10th June 2021)
- [13] Booij, N.R.R.C., Ris, R.C., & Holthuijsen, L.H. (1999). A third-generation wave model for coastal regions: 1. Model description and validation. *Journal of geophysical research: Oceans*, 104(C4), 7649-7666.
- [14] Gorelick, N., Hancher, M., Dixon, M., Ilyushchenko, S., Thau, D. and Moore, R. (2017), Google Earth Engine: Planetary-scale geospatial analysis for everyone, *Remote Sensing of Environment*, vol. 202, pp. 18-27. <https://doi.org/10.1016/j.rse.2017.06.031>
- [15] Luijendijk, A., Hagenaars, G., Ranasinghe, R., Baart, F., Donchyts, G. and Aarninkhof, S. (2018), The State of the World's Beaches, *Scientific reports*, vol. 8:6641. <https://doi.org/10.1038/s41598-018-24630-6>
- [16] Chen, B., Xiao, X., Li, X., Pan, L., Doughty, R., Ma, J., ... & Giri, C. (2017). A mangrove forest map of China in 2015: Analysis of time series Landsat 7/8 and Sentinel-1A imagery in Google Earth Engine cloud computing platform. *ISPRS Journal of Photogrammetry and Remote Sensing*, 131, 104-120.
- [17] Holdaway, A., Ford, M., & Owen, S. (2021). Global-scale changes in the area of atoll islands during the 21st century. *Anthropocene*, 33, 100282. <https://doi.org/10.1016/j.ancene.2021.100282>